Supporting information for:

Next-generation derivatization reagents optimized for enhanced product ion formation in photodissociation-mass spectrometry of fatty acids

Venkateswara R. Narreddula[a], Benjamin I. McKinnon[b], Samuel J. P. Marlton[b], David L. Marshall[c,d], Nathan R. B. Boase[a,d], Berwyck L. J. Poad[c,d], Adam J. Trevitt[b], Todd W. Mitchell[e,f], and Stephen J. Blanksby[a,c,d*]

[a]School of Chemistry and Physics, Science and Engineering Faculty, Queensland University of Technology, Brisbane, QLD 4000, AUSTRALIA

[b]Molecular Horizons and School of Chemistry and Molecular Bioscience, University of Wollongong, Wollongong, NSW 2522, AUSTRALIA

[c]Central Analytical Research Facility, Institute for Future Environments, Queensland University of Technology, Brisbane, QLD 4000, AUSTRALIA

[d]Centre for Materials Science, Queensland University of Technology, Brisbane, QLD 4000, AUSTRALIA

[d]School of Medicine, University of Wollongong, Wollongong, NSW 2522, AUSTRALIA

[e]Illawarra Health and Medical Research Institute, Wollongong, NSW 2522, AUSTRALIA

*Author to whom correspondence should be addressed: E-mail: stephen.blanksby@qut.edu.au (Stephen J. Blanksby)

1. Table of Content

2. Table of Tables

3. Table of Figures:

4. Table of Schemes

1. Experimental

1.1 Photodissociation action mass spectrometry

Photodissociation action spectra were performed using a linear quadrupole ion trap mass spectrometer (Thermo Fisher Scientific LTQ Velos) coupled with a pulsed, tuneable, laser (EKSPLA NT-342B). Experimental procedures have been explained previously in detail elsewhere.[1-3] Gas-phase ions were generated by an electrospray ionization (ESI) source where they are then focused towards a linear ion-trap and mass isolated. A single laser pulse irradiates the *m/z* selected ion at a time triggered by an electrical trigger-pulse aligned mechanical shutter to ensure a single photon packet irradiates the selected ion ensemble each isolation cycle. Photoproduct yield was calculated as the ratio of the photoproduct peak-area normalised to the total ion count. Laser power was attenuated to ~1 mW (0.05 mJ/pulse) with a motorized variable laser attenuator (Standa 10MVAA) and power normalised with a Gentec XLP12-3S-H2-D0 via an offline power scan. Reported photodissociation action spectra explore the mid-band UV region of 350-225 nm at a 1 nm resolution.

1.2 Computational calculations

Initial structural optimisations of derivative **5** and derivative **9** were undertaken in the ORCA/4.2.1 program package employing the density functional theory (DFT) M06-2X method and the def2-SVP basis set treating the iodine atom with an effective core potential (ECP).[4-8] All ground state energies are corrected for zero-point energy. Attempts to optimise multiple conformers converged to one of two structures for derivative **5** and one of three structures for derivative **9** as show in Figure S1. Structures were visualised using the Avogadro program.[9]

Lowest energy structures were re-optimised using SCS-CC2 with the def2-SVP basis set treating the iodine atom with an ECP in the TURBOMOLE (V7.2) program package.[7, 8, 10-12] These geometries were employed to calculate SCS-CC2 excitation energies with the def2-SVPD basis set. All coordinates were frozen except for the C-I bond which was extended to generate potential energy surfaces with vertical excitation energies calculated at the different C-I bond lengths using SCS-CC2/def2-SVPD. For compounds **5** and **9**, all states lower in energy than the first nσ* state at the equilibrium geometry were included in the potential energy surface while for compound **3**, all states lower in energy than the third ππ* state were included. For simplicity, only singlet states were calculated and higher energy states which remain higher in energy than the nσ* or πσ* states with C-I bond elongation were omitted. For all SCS-CC2 calculations,

the resolution of the identity approximation was employed.[13] Orbitals were visualised using the TmoleX18 program.[14]

Figure S1: Visualization of orbitals for important transitions in derivatives **3**, **5** and **9**.

Orbital visualization for transitions from ground state to excited state for (A) **3** (B) **5** and (C) **9**. The bright ππ* is populated after photon absorption, and the dark, unbound πσ* should drive I• loss. Presumably, the ππ* undergoes internal conversion to the πσ* state. Energies here are from the SCS-CC2/def2-SVPD level of theory and basis set using SCS-CC2/def2-SVP geometries. The energies of the ππ* for each compound are plotted in the action spectra with a 0.3 eV red-shift.

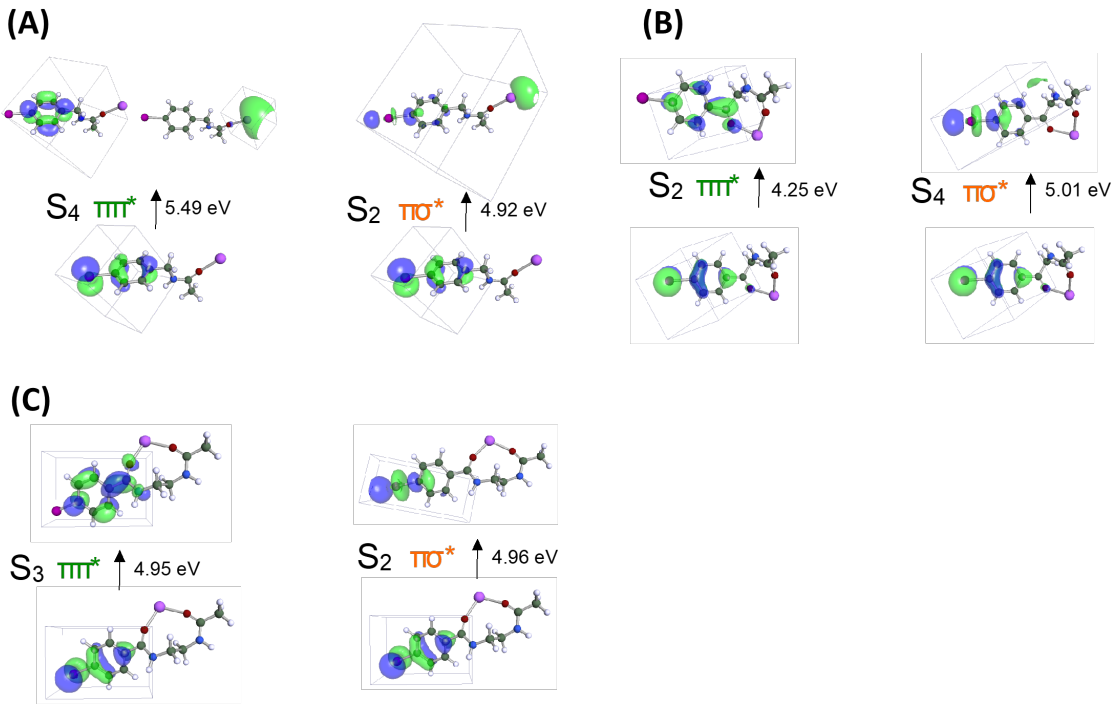

2. LC-MS methods

2.1 LC Method-1

Column: Acclaim™ C30, 150 mm × 2.1 mm, 3.0 µm (Thermo Fisher Scientific)

Column Temperature: 45 °C

Sample Diluent: Methanol

Mobile Phase A: Water with 0.1% formic acid

Mobile Phase B: Acetonitrile with 0.1% formic acid

Table S1: LC method-1 elution gradient

Time minutes)	Flow (mL min^{-1})	% Mobile Phase A	% Mobile Phase B
0.0	0.3	70	30
0.0	0.3	70	30
1.0	0.3	70	30
2.5	0.3	20	80
15.0	0.3	15	85
26.0	0.3	10	90
28.0	0.3	2	98
36.8	0.3	2	98
37.0	0.3	70	30
40.0	0.3	70	30

PD_{266} mass spectra of a mixture of 37 FAs derivatized with NIBA were acquired via targetted precursor ion mass selection in a segmented LC-MS run. The 40 min run time was partitioned into 10 time-based segments depending on the retention time of NIBA derivatized FA standards (see, Table S2). Each segment was then subdivided into 9-11 PD_{266} events based on how many derivatives eluted in that particular time segment. Within each segment a full scan mass spectrum was acquired, followed by sequentially-triggered PD_{266} mass spectra for each defined, $[M + Na]^+$ precursor ion mass. Typical ESI source parameters were: spray voltage +5.0 kV, capillary temperature 420 °C, tube lens voltage ~65 V, and capillary voltage 21 V. Nitrogen gas served as the sheath (set at 5 -10 arbitrary units), auxiliary and sweep gases (0 - 5 arbitrary units).

Table S2: Targeted photodissociation schedule for mixture of FA standards as NIBA derivatives.

The LC run time was divided into 10 segments based on the elution times of the FA standards derivatized with reagent **23** (**NIBA**). Each segment was programmed with 7-11 precursor ion masses corresponding to derivatized FAs eluting in that time window. Within each segment a full scan mass spectrum was taken, followed by photodissociation triggered sequentially for each defined precursor ion mass.

Segment	time (mins)	*m/z*	Event
1	0-7 min	Full scan	MS
		383.3	PD
		397.1	
		411	
		439.1	
		467.1	
		481.2	
		495.1	
		521.1	
		509.2	
2	7-7.9 mins	Full scan	MS
		439.1	PD
		467.1	
		481.2	
		495.1	
		521.1	
		509.2	
		535.1	
		597.2	
3	7.9-8.7mins	Full scan	MS
		481.2	PD
		495.1	
		521.1	
		509.2	
		535.1	
		597.2	
		523.2	
		573.3	
		623.3	
		549.2	
4	8.7-9.2mins	Full scan	MS
		495.1	PD
		521.1	
		509.2	
		535.1	
		597.2	
		523.2	
		573.3	
		623.3	
		549.2	
		599.2	
5	9.2-10.3 mins	Full scan	MS
		535.1	PD
		597.2	
		523.2	
		573.3	
		623.3	
		549.2	
		599.2	
		575.3	
		537.2	
		601.3	
		509.2	
6	10.6-12.2 mins	Full scan	MS
		523.2	PD
		573.3	
		623.3	
		549.2	
		599.2	
		575.3	
		537.2	
		601.3	
		551.2	
		577.3	
		603.2	
7	12.2-15.2 mins	Full scan	MS
		537.2	PD
		601.3	
		551.2	
		577.3	
		603.2	
		565.2	
		579.3	
		605.2	
8	15.218.2 mins	Full scan	MS
		551.2	
		577.3	
		603.2	
		565.2	PD
		579.3	
		605.2	
		631.3	
		593.3	
9	18.2-25.2 mins	Full scan	MS
		579.3	PD
		605.2	
		631.3	
		593.3	
		633.3	
		607.3	
		621.3	
10	25.2-40.0 mins	Full scan	MS
		631.3	PD
		593.3	
		633.3	
		607.3	
		621.3	
		661.3	
		635.3	
		649.3	
		663.3	

2.2 LC Method-2

Column: Acclaim™ C30, 150 mm × 2.1 mm, 3.0 µm (Thermo Fisher Scientific)

Column Temperature: 45 °C

Sample Diluent: Methanol

Mobile Phase A: Water with 0.1% formic acid

Mobile Phase B: Acetonitrile with 0.1% formic acid

UV detection wavelengths: 254 nm, 266 nm

Simultaneous acquisition of UV absorption and PD mass spectra is achieved by splitting the column eluent, with the split ratio controlled by the length and diameter of 2 capillaries attached to a post-column tee junction. In this case, 10% of the flow is injected into the mass spectrometer for acquisition of MS, and PD spectra, while the remaining 90% passes through the photodiode array for UV absorption measurements by PDA detector from 190–800 nm range.

Table S3: LC Method 2 Gradient

Time (minutes)	Flow (mL/min)	% Mobile Phase A	% Mobile Phase B
0:0	0.3	70	30
2:0	0.3	70	30
4:0	0.3	25	75
12:0	0.3	05	95
17:0	0.3	05	95
17:1	0.3	70	30
20:0	0.3	70	30

3. Additional mass spectrometry data

Figure S2: Effect of the adducting cation on PD_{266} for 4-iodobenzylamine derivatives of FA 18:1(9*Z*).

PD spectra (λ = 266 nm) of [**3** + X]$^+$ where: (A) X = H (*m/z* 498); (B) X = Li (*m/z* 504); C) X = Na (*m/z* 520); and (D) X = K (*m/z* 536). Sample injected *via* direct infusion. Spectra represent an average of 80 scans. Spectrum (B) was acquired by addition of 0.1 mM lithium acetate, and Spectrum (D) was acquired by addition of potassium iodide to the infusion solution. 'NL' represents the ion count for the base peak.

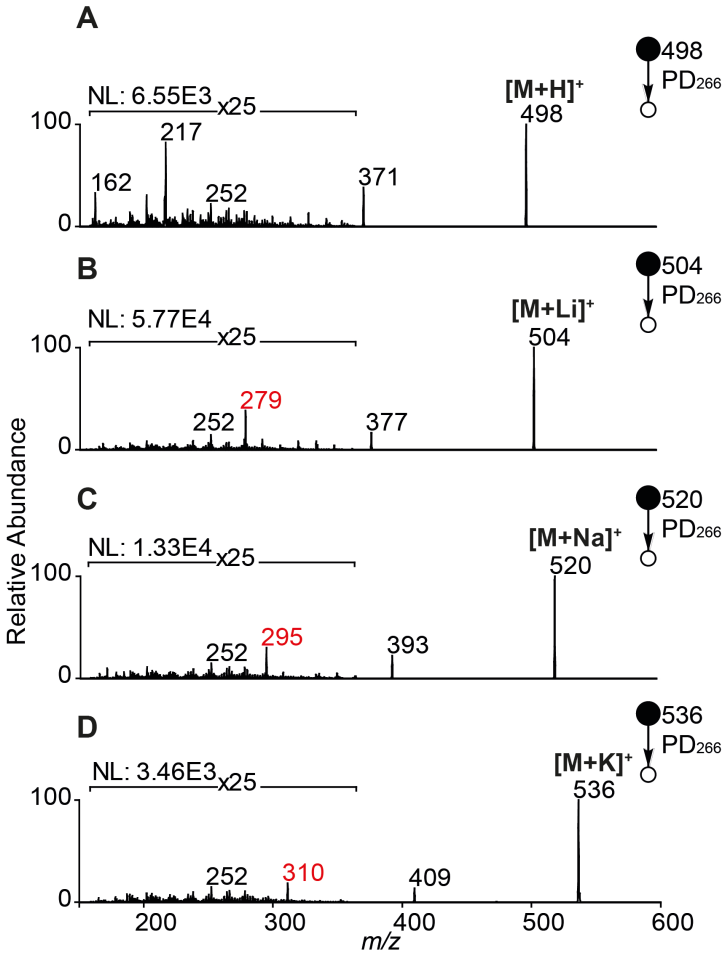

Figure S3: Effect of the adducting cation on PD_{266} conversion for 4-iodobenzylamine derivatives of FA 18:1(9*Z*).

Normalized abundance of product ions from PD_{266} mass spectra of [**3** + X]$^+$ where: (A) X = H (*m/z* 498); (B) X = Li (*m/z* 504); (C) X = Na (*m/z* 520); and (D) X = K (*m/z* 536). Bars show mean and standard deviation across 80 individual scans.

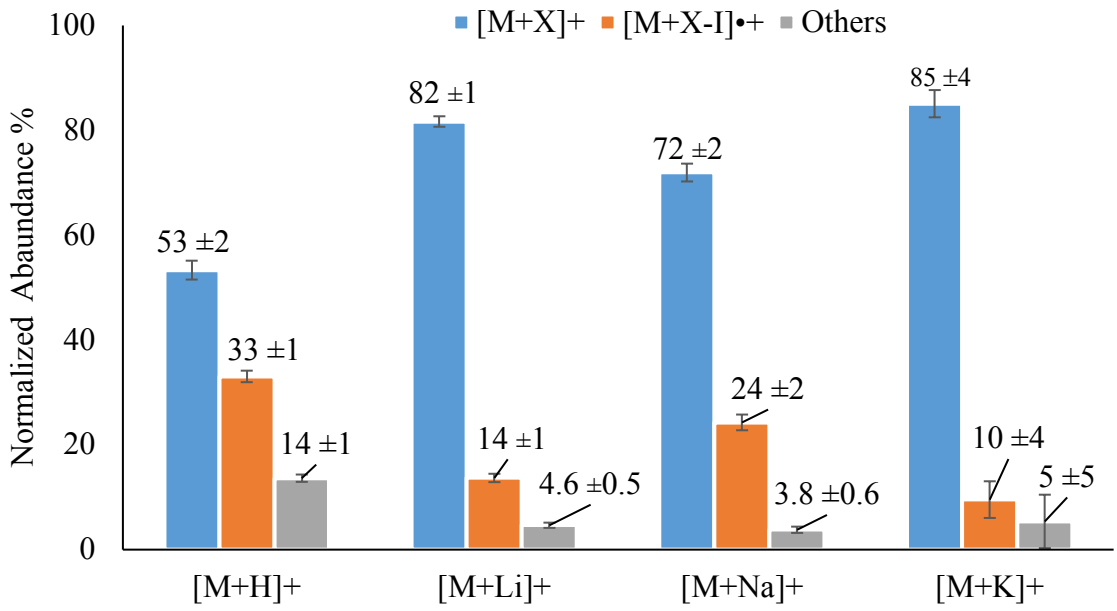

Figure S4: Effect of the adducting cation on PD_{266}/CID spectra of 4-iodobenzylamine derivatives of FA 18:1(9*Z*).

PD/CID (MS^3) mass spectra of $[\mathbf{3} + X - I]^{\bullet+}$ where: (A) X = H (*m/z* 371); (B) X = Li (*m/z* 377); (C) X = Na (*m/z* 393); and (D) X = K (*m/z* 409). Spectra represent an average of 80 scans, acquired with a normalized collision energy of 15 for the CID step. 'NL' represents the ion count for the base peak.

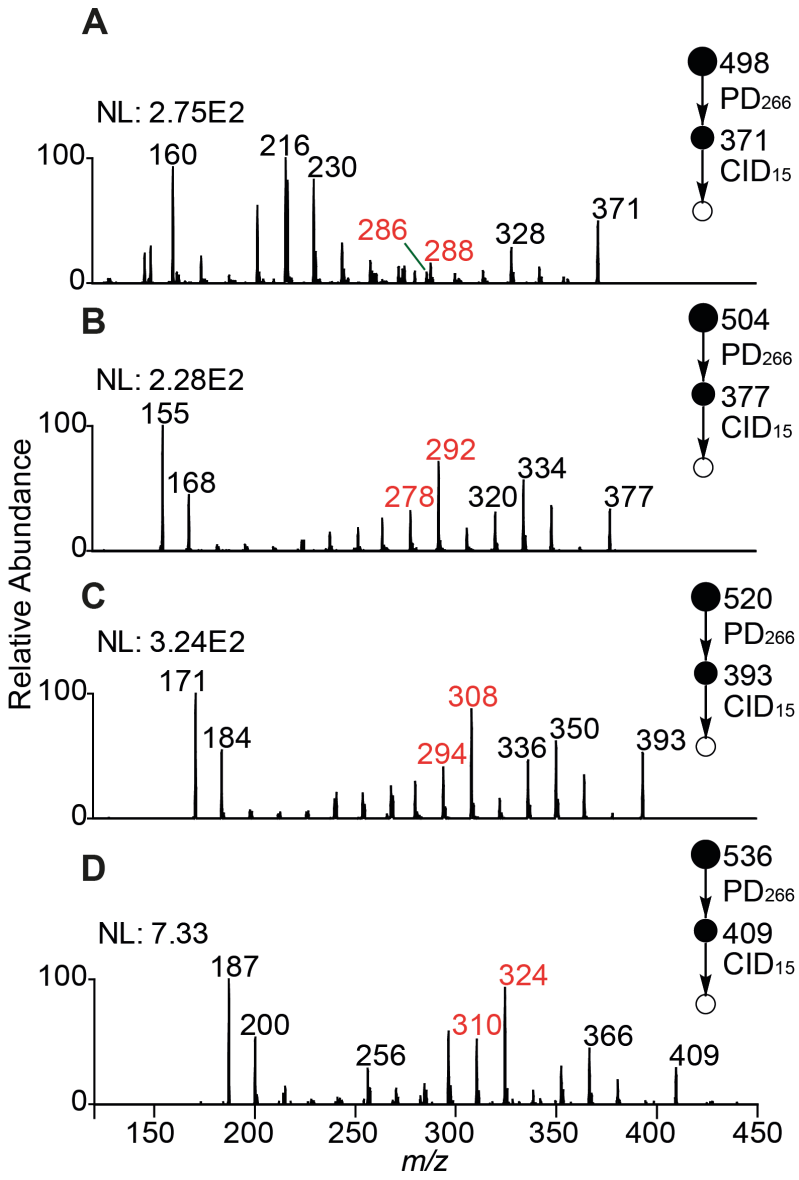

Figure S5: PD_{266} and PD_{266}/CID mass spectra of FA 18:1(9*Z*) derivatized with 4-iodobenzylamine and 4-iodobenzyl alcohol.

PD_{266} (MS^2) mass spectra of $[M + Na]^+$ ions of FA 18:1(9*Z*) derivatized with (A) 4-iodobenzylamine (*m/z* 520, **3**) and (B) 4-iodobenzyl alcohol (*m/z* 521, **4**). PD_{266}/CID (MS^3) mass spectra of $[M + Na - I]^{\bullet+}$ of FA 18:1(9*Z*) derivatized with (C) 4-iodobenzylamine (**3**) and (D) 4-iodobenzyl alcohol (**4**). Sample injected in methanolic solution *via* direct infusion. Spectra represent an average of 80 scans, acquired with a normalized collision energy of 15. 'NL' represents the ion count for the base peak.

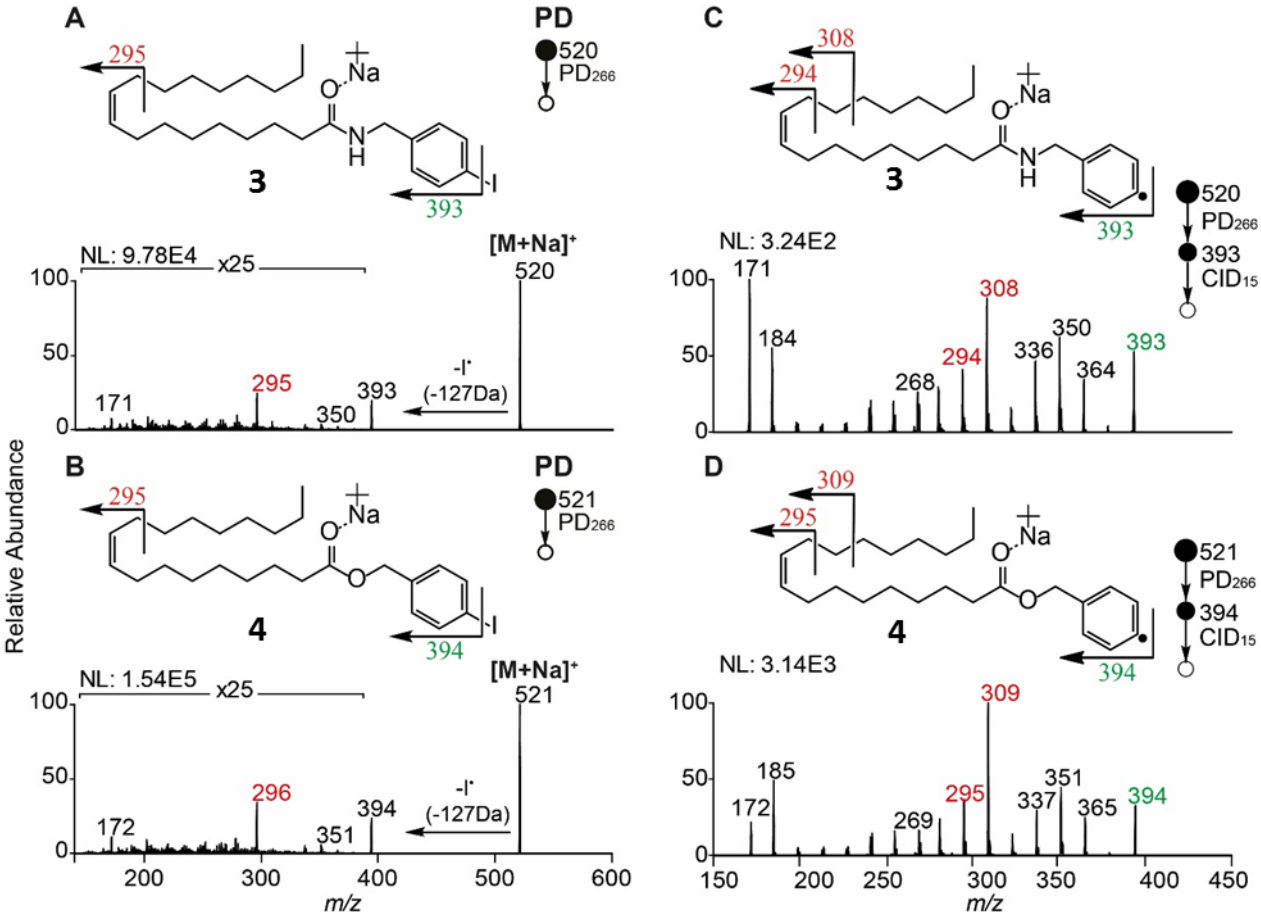

Figure S6: PD_{266}/CID mass spectra of FA 18:1(9*Z*) derivatized with different reagents.

PD_{266}/CID mass spectra of FA 18:1(9*Z*) derivatized to yield the structures (A) **4**, (B) **5**, (C) **6**, (D) **7**, (E) **8** and (F) **9**. Methanolic solutions of each sample were injected *via* direct infusion ESI. Spectra represent an average of 80 scans and were acquired with a normalized collision energy of 17. 'NL' represents the ion count for the base peak.

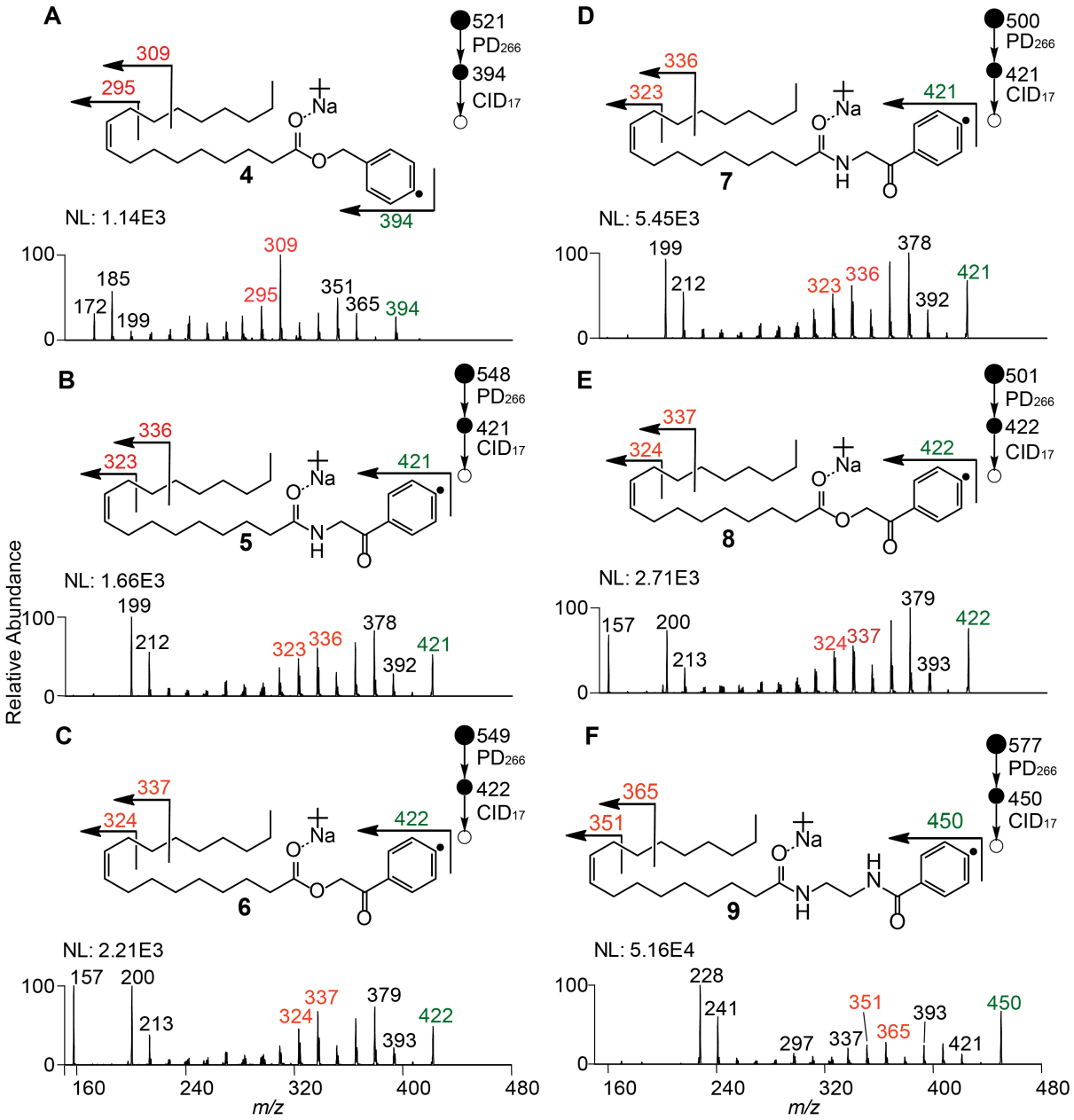

Figure S7: LC-UV absorption of derivatives **5**, **7** and **9**.

To obtained these data 20 µL of **5**, **7** and **9** (100 µM in methanol) were injected onto the C30 column and eluted using LC method 2. The column eluent was split with 10% diverted to the mass spectrometer and 90% delivered to the photodiode array (PDA). The solution phase UV absorption of **5**, **7** and **9** was measured using PDA detector between 200-800 nm wavelengths. UV absorption was measured simultaneously at (A) 230 nm, (B) 254 nm, (C) 266 nm and (D) 280 nm and the solvent mixture was 95:5 % acetonitrile and water mixture with 0.1% formic acid additive at the time of elution.

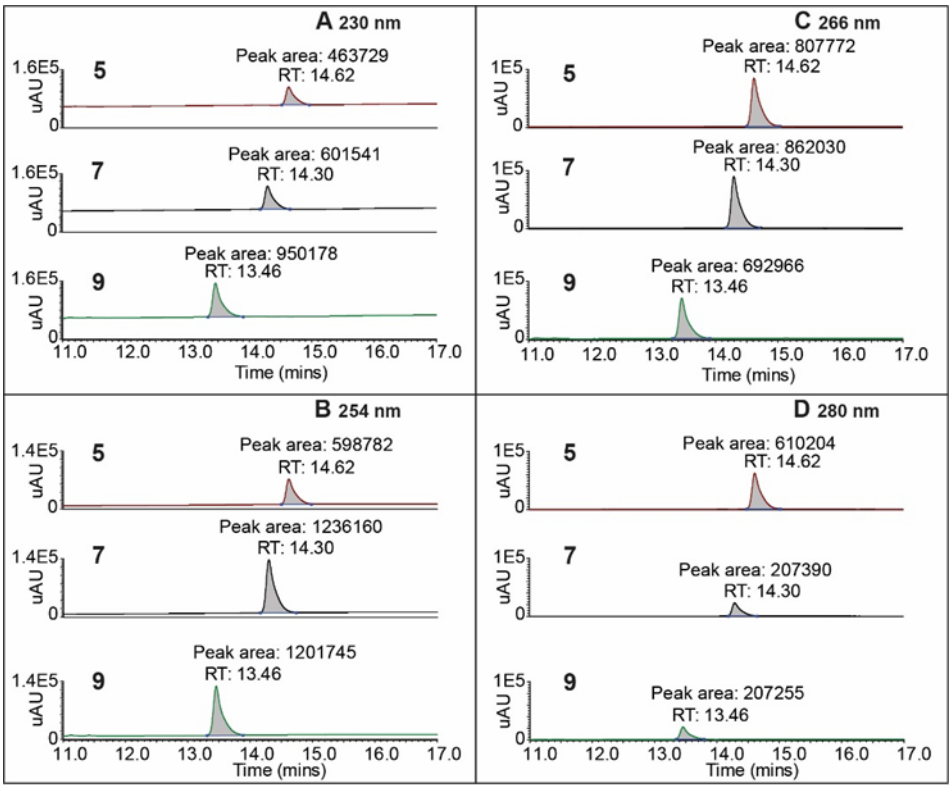

Figure S8: UV absorption spectra of FA 18:1(9*Z*) as derivatives **5**, **7** and **9**.

The solution phase UV absorption of **5**, **7** and **9** was measured using PDA detector between 200-800 nm wavelength on LC-UV-MS run. The absorption maxima are indicated at the apex of each absorption feature. NL (or normalization limit) is reported by the instrument control software and refers to the absolute absorption to which the absorption is normalized in the region of interest.

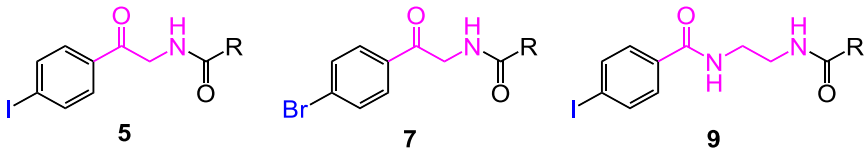

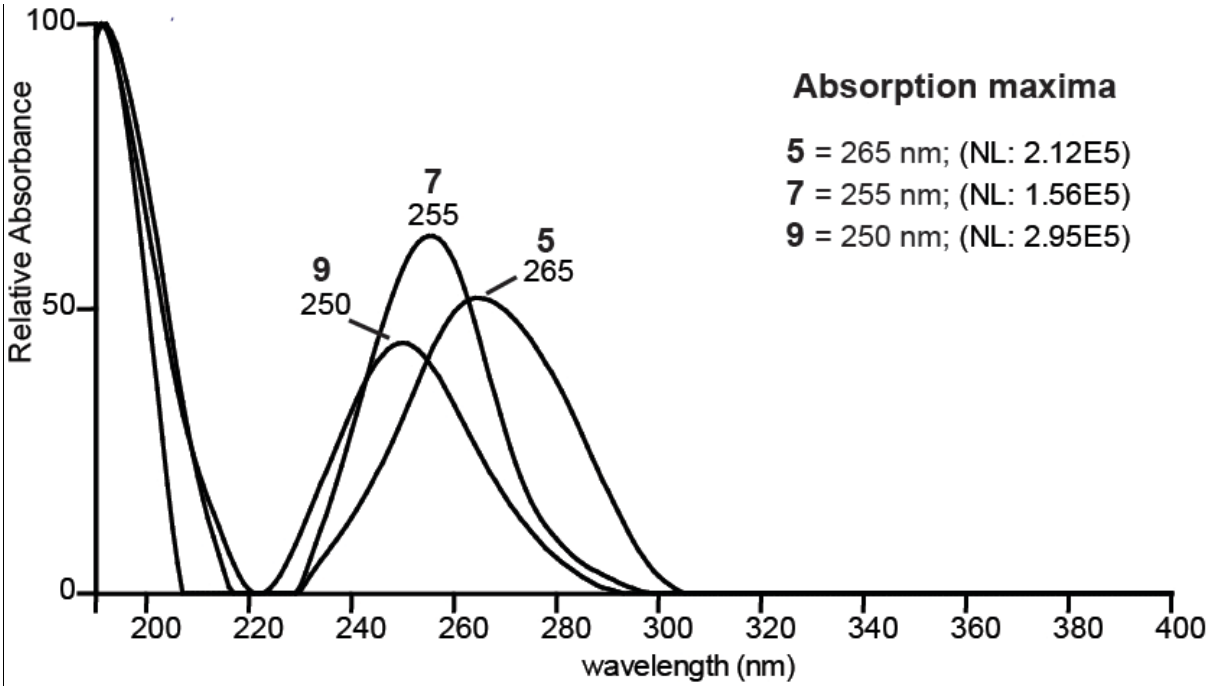

Figure S9: Total ion abundance of the ESI-CID (MS^2, NCE = 0), ESI-PD_{266} (MS^2) and ESI-PD_{266}/CID (MS^3, NCE = 17) mass spectra of **9**.

The absolute product ion abundance from ESI-MS, ESI-PD (MS^2) and ESI-PD/CID (MS^3) mass spectra acquired from NIBA derivatized FA 18:1(9*Z*), **9**. The data represent the average ion counts from triplicate injections where the error bars represent 1 standard deviation from the mean.

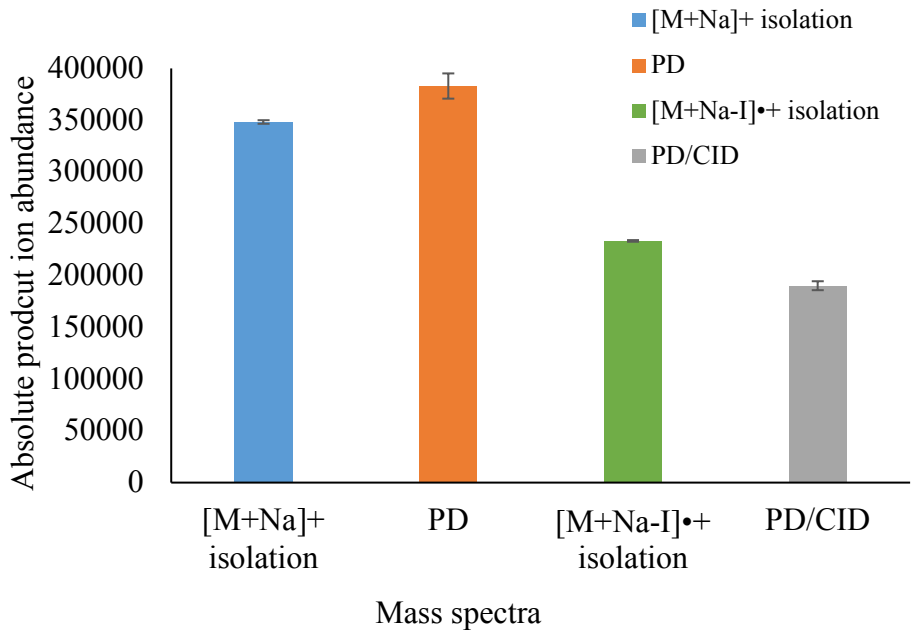

Figure S10: Extracted ion chromatograms of $[M + Na - I]^{\bullet+}$ ions from the mixture of FA standards as NIBA derivatives.

Extracted ion LC-PD_{266} traces of (A) saturated FAs; (B) monounsaturated FAs; (C & D) polyunsaturated FAs. LC traces are extracted for PD_{266} radical cation ($[M + Na - I]^{\bullet+}$) using LC-MS method 1.

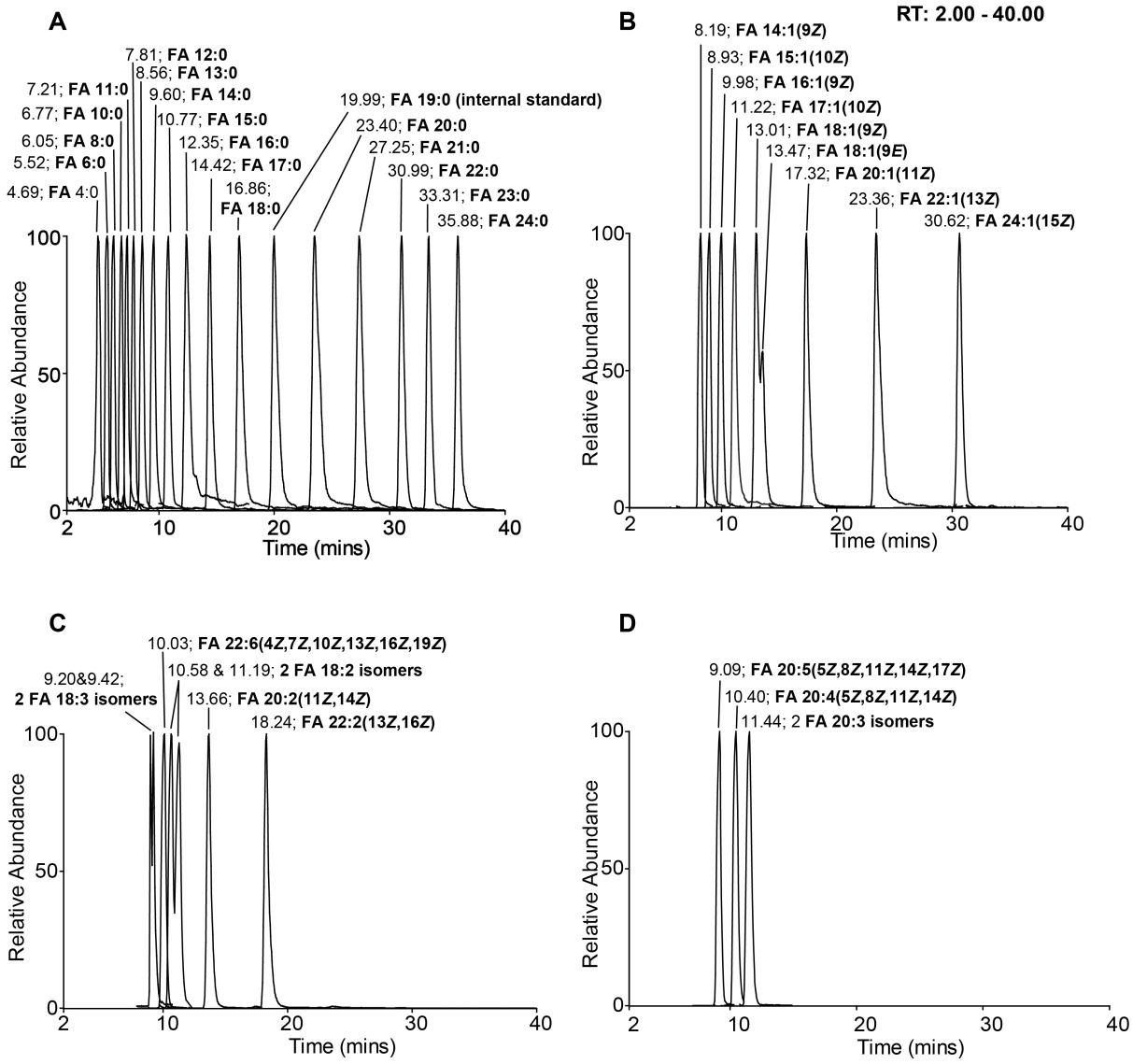

Table S4: LC retention times of 37 mix FA standards as NIBA derivatives.

LC-MS data acquired using LC Method 1 on a C30 column. Retention times derived from the apex of the chromatographic peak in the respective extracted ion chromatogram for the PD_{266} transition corresponding to loss of iodine, *i.e.*, $[M + Na - I]^{+\bullet}$.

S. No.	Fatty acid	RT (mins)	S. No.	Fatty acid	RT (mins)
1	FA 4:0	4.69	20	FA 18:1(9Z)	13.01
2	FA 6:0	5.52	21	FA 18:1(9E)	13.47
3	FA 8:0	6.05	22	FA 18:0	16.86
4	FA 10:0	6.77	23	FA 19:0 (internal standard)	19.99
5	FA 11:0	7.21	24	FA 20:5(5Z,8Z,11Z,14Z,17Z)	9.09
6	FA 12:0	7.81	25	FA 20:4(5Z,8Z,11Z,14Z)	10.40
7	FA 13:0	8.56	26	FA 20:3(11Z,14Z,17Z) FA 20:3(8Z,11Z,14Z)	11.44
8	FA 14:1(9Z)	8.19	27	FA 20:2(11Z,14Z)	13.66
9	FA 14:0	9.60	28	FA 20:1(11Z)	17.32
10	FA 15:1(10Z)	8.93	29	FA 20:0	23.40
11	FA 15:0	10.77	30	FA 21:0	27.25
12	FA 16:1(9Z)	9.98	31	FA 22:6(4Z,7Z,10Z,13Z,16Z,19Z)	10.03
13	FA 16:0	12.35	32	FA 22:2(13Z,16Z)	18.24
14	FA 17:1(10Z)	11.22	33	FA 22:1(13Z)	23.86
15	FA 17:0	14.42	34	FA 22:0	30.99
16	FA 18:3(9Z,12Z,15Z)	9.20	35	FA 23:0	33.31
17	FA 18:3(6Z,9Z,12Z)	9.42	36	FA 24:1(15Z)	30.62
18	FA 18:2(9Z,12Z)	10.58	37	FA 24:0	35.88
19	FA 18:2(9E,12E)	11.19			

Figure S11: Normalized product ion abundances from PD_{266} mass spectra of a standard mixture of FAs as NIBA derivatives.

Each bar in the bar graph represents the averaged normalized abundance of product ions obtained from the triplicates of PD spectra of individual FA (from 37 mix) derivatized with NIBA derivatization reagent. In each bar: blue represents the residual $[M + Na]^+$ precursor ions; orange represents the contribution of the the $[M + Na - I]^{\bullet+}$ product ion while; grey represents the remaining products of photolysis arising from radical-directed dissociation of the FA itseld. LC-MS data were acquired using LC-method 1 and all product ion abundances represent the average of 4 scans.

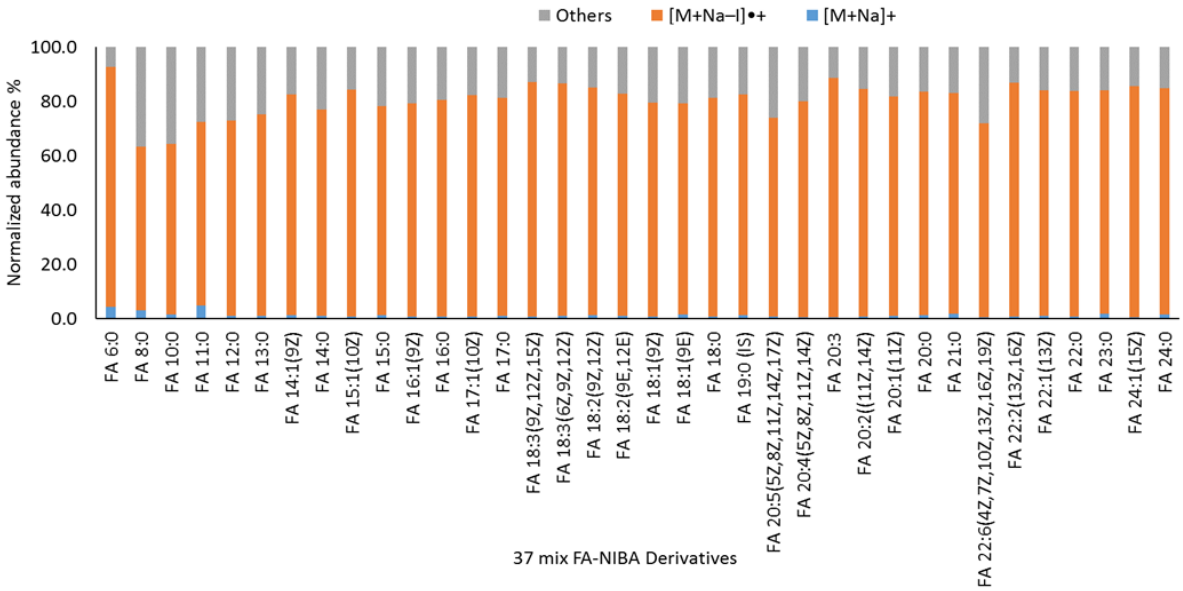

Figure S12: Mass spectra arising from the gas phase reaction of $[M + Na - I]^{\bullet+}$ ions, formed by PD_{266} of NIBA derivatized FA 6:0 and FA 8:0, with dioxygen.

Mass spectra of reaction between $[M + Na - I]^{\bullet+}$ ions formed by PD_{266} of (A) FA 6:0-NIBA (*m/z* 284) and (B) FA 8:0-NIBA (*m/z* 312) with dioxygen obtained 1000, 2000, 4000, 6000, 8000 and 10000 ms after isolation. The mass spectra are plotted from *m/z* 240-340 for FA 6:0-NIBA (*m/z* 284) and from *m/z* 270-370 for FA 8:0-NIBA (*m/z* 312) and each represent an average of 12 individual scans. The mass acquired via direct infusion by injecting 25 µL of 0.5 µM methanolic solution of the NIBA derivatized 37 mix of FAs.

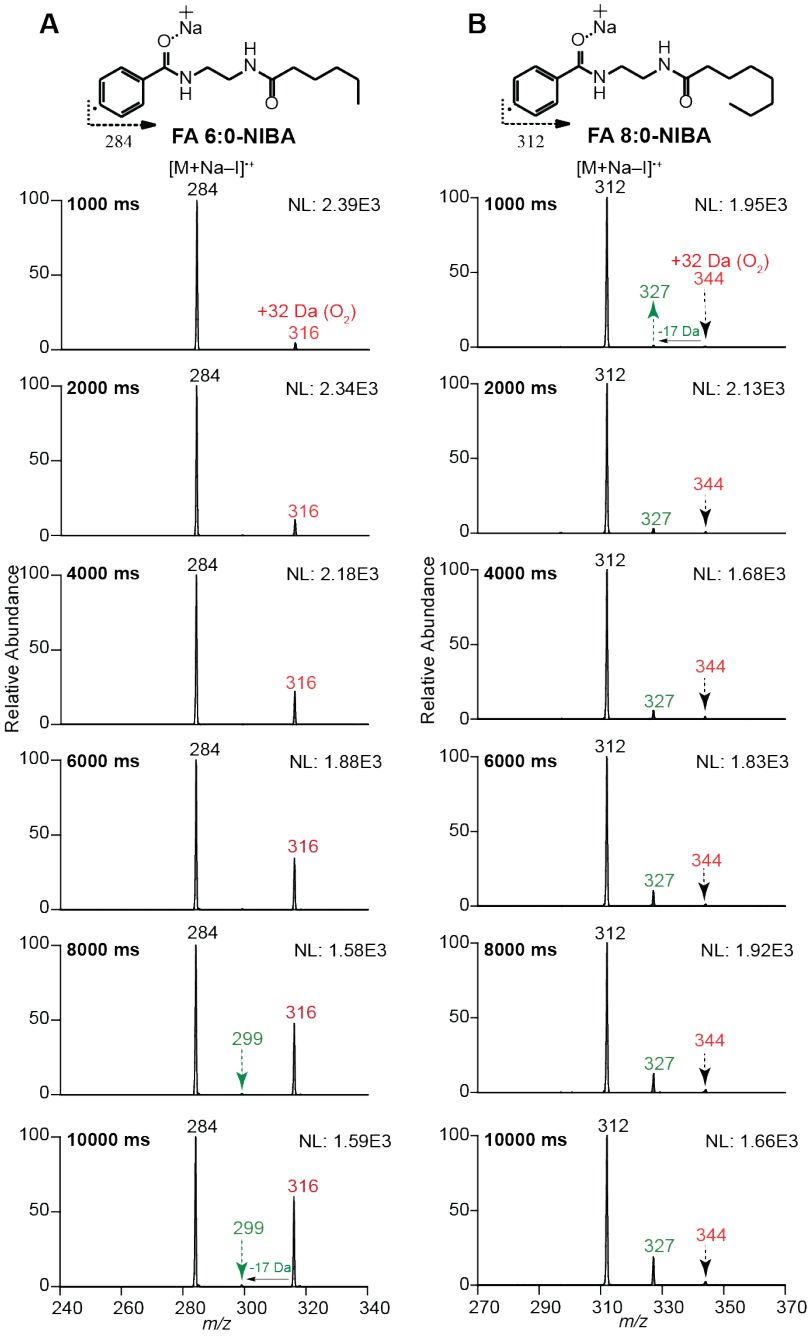

4. Synthesis of derivatization reagents

4.1 Materials

Reagent grade starting materials were used for synthesis. (2-iodophenyl)methanamine (**10**), 3-Iodobenzylamine hydrochloride (**11**), 4-iodobenzylamine hydrochloride (**12**), 2,4'-dibromo-acetophenone (**13**), 2-amino-4′-bromoacetophenone hydrochloride (**14**), 4-iodoacetophenone (**15**), 4-iodobenzoic acid (**21**), 4-iodobenzyl alcohol, tetrabutylammonium hydroxide (TBAOH) solution (40 wt. % in H_2O), bromine, 1,2-diaminoethane (**19**), 1,3,5,7-tetraazaadamantane, and 1,2-diaminoethane were purchased from Sigma-Aldrich (Sydney, Australia). 1-[Bis(dimethylamino)methylene]-1*H*-1,2,3-triazolo[4,5-*b*]pyridinium 3-oxide hexafluorophosphate (HATU), di-*tert*-butyl dicarbonate (Boc_2O), and trifluoroacetic acid (TFA) were purchased form Tokyo Chemical Industry, Japan. Analytical grade (AR) ethanol (EtOH), AR grade anhydrous N, N-dimethylformamide (DMF) were purchased from Sigma-Aldrich Australia. Laboratory reagent (LR) grade solvents used for purification and synthesis of derivatization reagents, which are hexanes, ethyl acetate (EtOAc), MeOH, dichloromethane (DCM), methyl tertiary butyl ether (MTBE, HPLC grade) and chloroform were purchased from Chem-Supply Australia (as Thermo Fisher Scientific, Scoresby, Australia).

All the NMR experiments were measured by using Bruker Topspin 3.5, 600 MHz instrument. NMR spectra were processed using MestreNova software. Melting range of synthesized compounds is measured using Gallenhamp melting point apparatus.

5. Synthesis of derivatization reagents and derivatives

5.1 Synthesis of 2-amino-1-(4-iodophenyl)ethan-1-one hydrochloride (18)

Scheme S1: 2-amino-1-(4-iodophenyl)ethan-1-one hydrochloride (**18**).

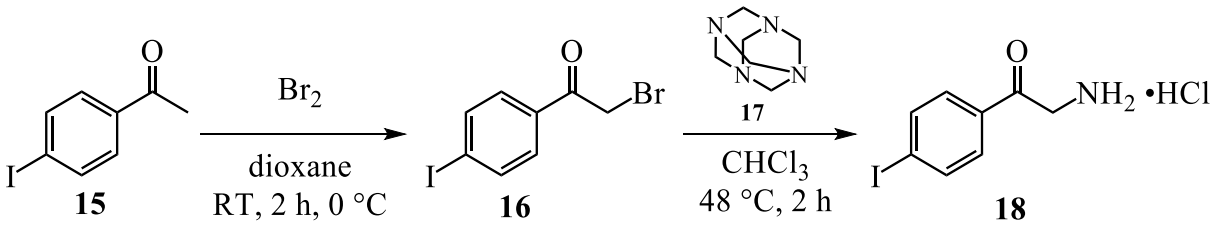

2-Bromo-1-(4-iodophenyl)ethan-1-one (**16**):

Compound **16** was synthesized by adapting a literature procedure.[15] To an ice cold solution of 4-iodoacetophenone (**15**, 1.0 g, 4.08 mmol, 1 equiv.) in dioxane, 0.25 mL of bromine (0.23 mL, 4.48 mmol, 1.1 equiv.) was added dropwise at 0 °C. The resulting mixture was stirred at room temperature for 2 h. The reaction mixture was concentrated under vacuum. The residue was diluted with water (10 mL) and extracted with DCM (2 x 10 mL). The organic layer was dried over Na_2SO_4 and concentrated under vacuum. The residue was purified by column chromatography on silica gel by eluting with hexane : EtOAc to give 2-bromo-1-(4-iodophenyl)ethan-1-one (**16**, 500 mg, 36%) as an off-white solid. ^{1}H NMR ($CDCl_3$, 600 MHz) δ (ppm): δ 7.92 – 7.81 (m, 2H), 7.74 – 7.64 (m, 2H), 4.39 (s, 2H). Melting range: 92-94 °C.

2-Amino-1-(4-iodophenyl)ethan-1-one hydrochloride (**18**):

Compound **18** was synthesized by adapting a previously reported procedure.[16] Intermediate **16** (45 mg, 0.13 mmol, 1.0 equiv.) and hexamethylenetetramine (**17**, 22.6 mg, 0.16 mmol, 1.2 equiv.) was dissolved in chloroform (1.0 mL) at room temperature. The resulting mixture was heated to 48 °C for 4 h, then cooled to room temperature. The white solid obtained was filtered, washed with 0.2 mL EtOH and dried under vacuum. The solid was dissolved in 0.4 mL EtOH and 0.12 mL concentrated HCl was added dropwise. The mixture was stirred at room temperature for 22 h, filtered, washed with 0.2 mL deionized water and dried in a vacuum oven for 2 h at 40 °C to give title compound (**18,** 40 mg, 97%) as a white solid. ^{1}H NMR (600 MHz, DMSO-d_6) δ 8.35 (s, 3H), 8.03 – 7.98 (m, 2H), 7.80 – 7.75 (m, 2H), 4.57 (s, 2H) (Figure S14). ESI-MS calculated for $C_8H_9INO^+$ $[M\text{-}Cl]^+$ *m/z* 261.9723, found *m/z* 261.9721 (Δ = 0.8 ppm) (Figure S15). Melting range: 272-275 °C.

5.2 Synthesis of TFA salt of *N*-(2-aminoethyl)-4-iodobenzamide (NIBA, 23)

Scheme S2: Synthesis of TFA salt of *N*-(2-aminoethyl)-4-iodobenzamide (**23**):

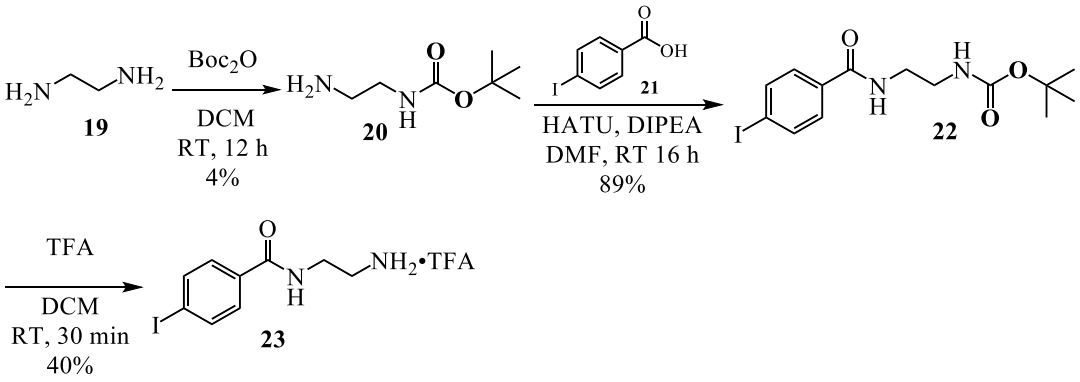

Tert-butyl (2-aminoethyl)carbamate (**20**):

Intermediate **20** was synthesized by adapting a procedure reported elsewhere.[17] 1,2-Diaminoethane (**19**; 1.0 g, 16.6 mmol 1.0 equiv.) was added to a 25 mL round-bottom flask containing DCM (5 mL) and the resulting solution was cooled to 0 °C. To this, solution of Boc_2O (0.6 g, 2.7 mmol, 0.16 equiv.) in DCM (3.6 mL) was added dropwise over 20 min with stirring at 0 °C. The resulting mixture was then warmed and stirred room temperature for 12 h. After the reaction time mixture was filtered to remove the white precipitate. The filtrate was concentrated under vacuum to remove excess 1,2-diaminoethane and DCM. The residue was then dissolved in EtOAc (30 mL), washed with saturated Na_2CO_3 (2 x 20 mL) followed by brine. The organic layer was dried with anhydrous Na_2SO_4 followed by filtration. Solvent was removed by rotary evaporation and the residue dried under vacuum to give a colourless oil, which was purified by silica gel column chromatography eluting with 5% MeOH : DCM to afford compound **20** (100 mg, 4%) as colourless oil. ^{1}H NMR ($CDCl_3$, 600 MHz), δ (ppm): 4.88 (s, 1H), 3.49 (s, 2H), 3.20-3.17 (m, 2H), 2.82-2.80 (m, 2H), 1.44 (s, 9H) (Figure S15: Positive mode ESI-HRMS spectrum of 2-amino-1-(4-iodophenyl)ethan-1-one hydrochloride (**18**)

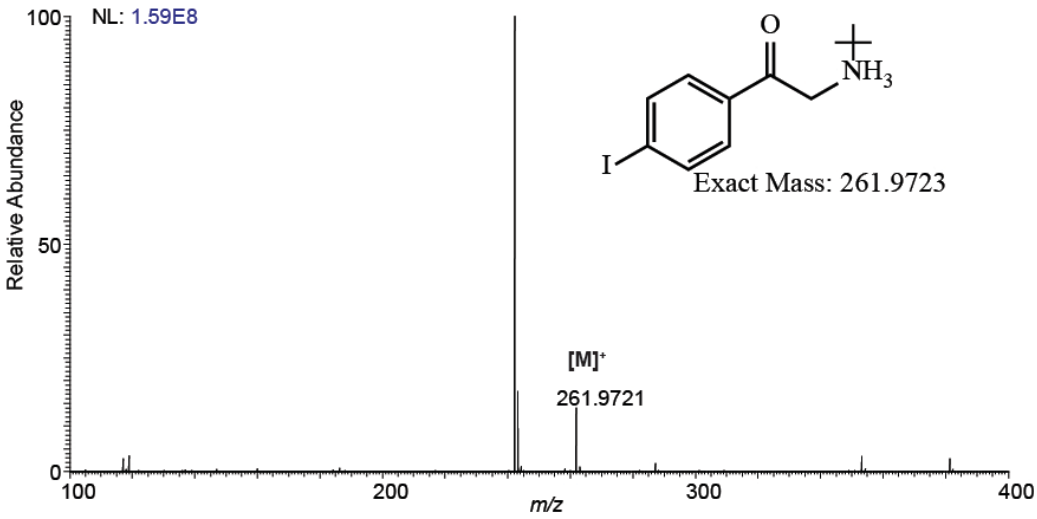
NL: 1.59E8
100
50
0
Relative Abundance
100
200
300
400
m/z
[M]+
261.9721
O
NH3
I
Exact Mass: 261.9723

Figure S16).

Tert-butyl (2-(4-iodobenzamido)ethyl)carbamate (**22**):

Compound **22** was synthesized by adapting procedure reported elsewhere.[18] To a solution of 4-iodobenzoic acid (**21**, 100 mg, 0.40 mmol, 1.0 equiv.) dissolved in DMF (0.5 mL), was added **20** (70 mg; 0.44 mmol, 1.1 equiv.) and HATU (230 mg; 0.60 mmol, 1.5 equiv.) followed by DIPEA (0.16 mL, 1.00 mmol, 2.5 equiv.) dropwise at room temperature. The mixture was stirred at room temperature for 16 h. The reaction mixture was poured into ice water and stirred for 10 min. The solid obtained was filtered and washed with deionised water (2 mL). The solid was dried under vacuum to give *tert*-butyl (2-(4-iodobenzamido)ethyl)carbamate (**22,** 140 mg, 89%) as an off-white solid. ^{1}H NMR ($CDCl_3$, 600 MHz) δ (ppm): 7.79 – 7.76 (m, 2H), 7.56 – 7.55 (m, 2H), 4.95 (brs, 1H), 3.55 – 3.52 (m, 2H), 3.49 (brs, 1H) 3.42 – 3.40 (m, 2H), 1.43 (s, 9H) (Figure S17). ESI-MS calculated for $C_{14}H_{20}IN_2O_3^+$ is *m/z* 391.0513, found *m/z* 391.0507 9 (Δ = 1.5 ppm) (Figure S 18); Melting range: 120-123 °C.

TFA salt of N-(2-aminoethyl)-4-iodobenzamide (NIBA, **23**):

To a solution of *tert*-butyl (2-(4-iodobenzamido)ethyl)carbamate (**22**, 140 mg, 0.35 mmol) in DCM (5 mL), was added trifluoroacetic acid (0.5 mL) and the resulting mixture was stirred at room temperature for 30 min. The reaction mixture was concentrated under vacuum, the residue obtained was triturated with toluene (2 x 2 mL) and dried under vacuum. The residue was taken in DCM and the precipitate was removed by filtration. Drying the precipitate under vacuum gave TFA salt of *N*-(2-aminoethyl)-4-iodobenzamide (**23**, 55 mg, 40%) as an off-white solid. ^{1}H NMR (DMSO-d_6, 500 MHz) δ 8.68 (d, J = 5.5 Hz, 1H), 7.88 (d, J = 8.5 Hz, 2H), 7.82 (s, 3H), 7.65 (d, J = 8.5 Hz, 2H), 3.49 (q, J = 6.1 Hz, 2H), 2.98 (h, J = 5.7 Hz, 2H) (Figure S19). ESI-MS calculated for $C_9H_{12}IN_2^+$ $[M\text{-}CF_3COO]^+$ *m/z* 290.9989, found *m/z* 290.9993 (Δ = 1.4 ppm) (Figure S20).

6. Characterization data for synthesized derivatization reagents

Figure S13: ^{1}H NMR spectrum of 2-bromo-1-(4-iodophenyl)ethan-1-one (**16**).

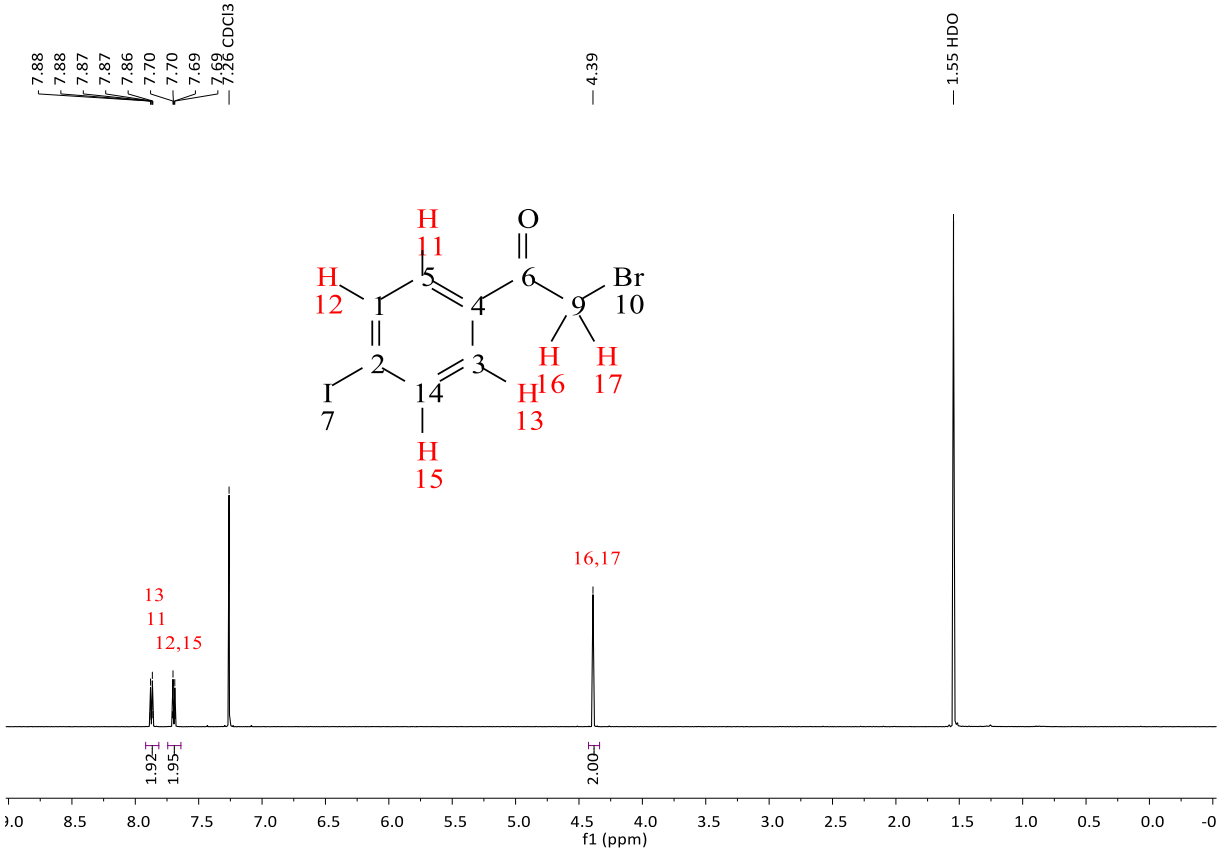

Figure S14: ^{1}H NMR spectrum of 2-amino-1-(4-iodophenyl)ethan-1-one hydrochloride (**18**).

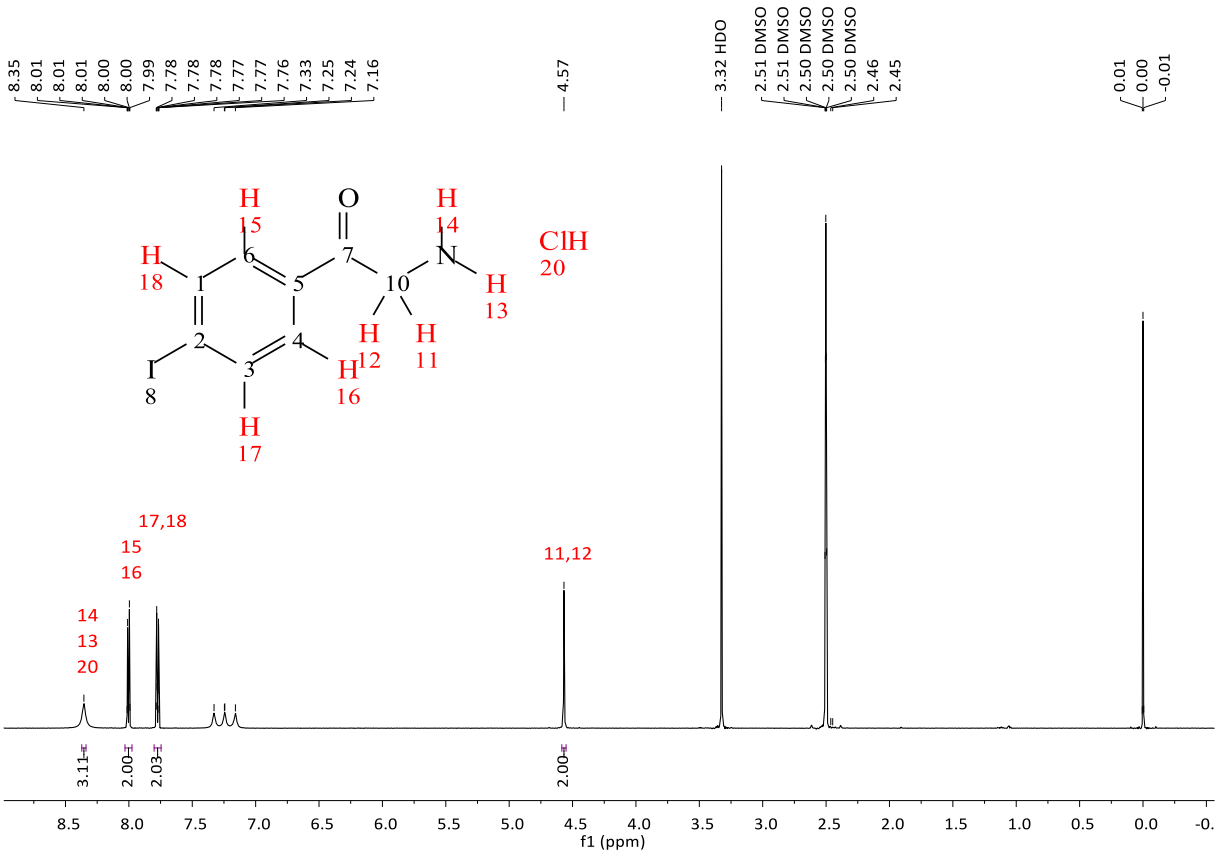

Figure S15: Positive mode ESI-HRMS spectrum of 2-amino-1-(4-iodophenyl)ethan-1-one hydrochloride (**18**)

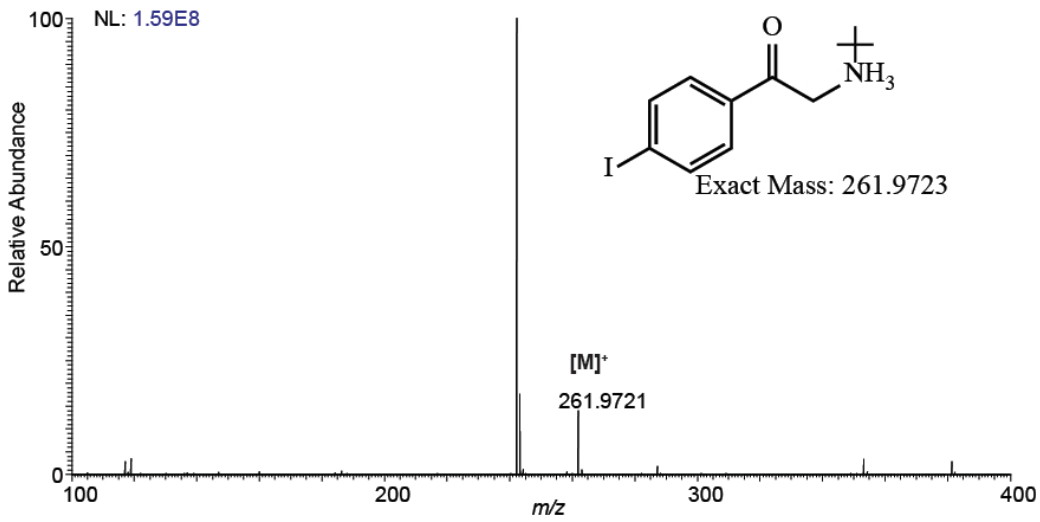

Figure S16: ^{1}H NMR spectrum of *tert*-butyl (2-aminoethyl)carbamate (**20**).

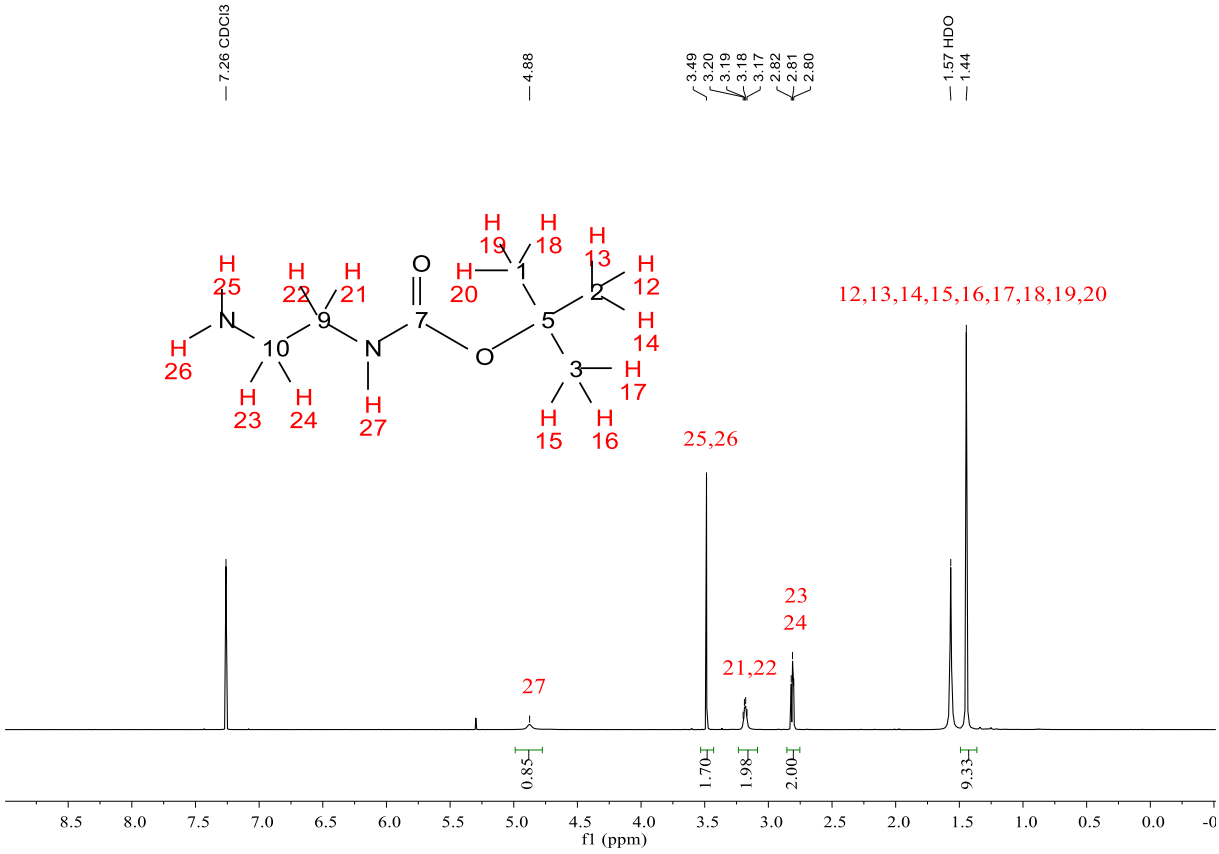

Figure S17: ^{1}H NMR spectra of *tert*-butyl (2-(4-iodobenzamido)ethyl)carbamate (**22**).

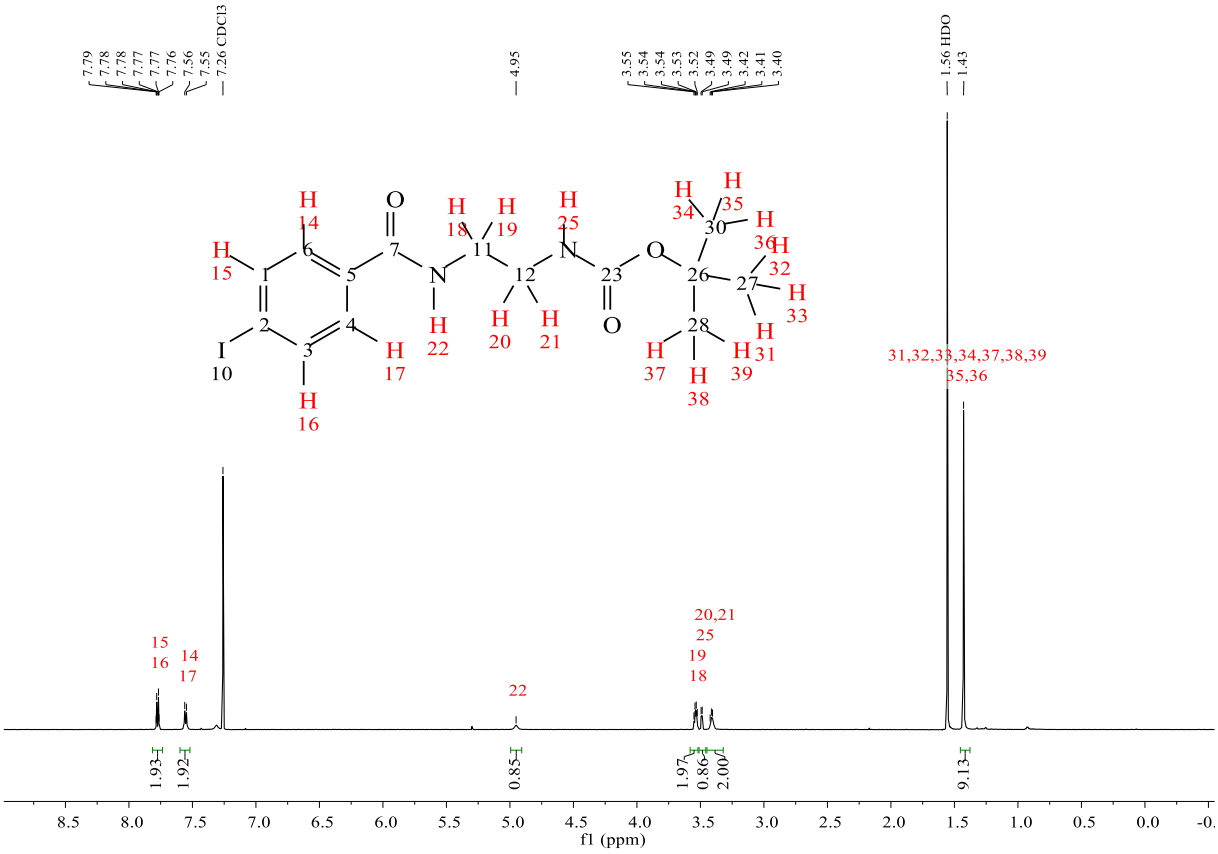

Figure S 18: Positive mode ESI-HRMS spectrum of *tert*-butyl (2-(4-iodobenzamido)ethyl)carbamate (**22**).

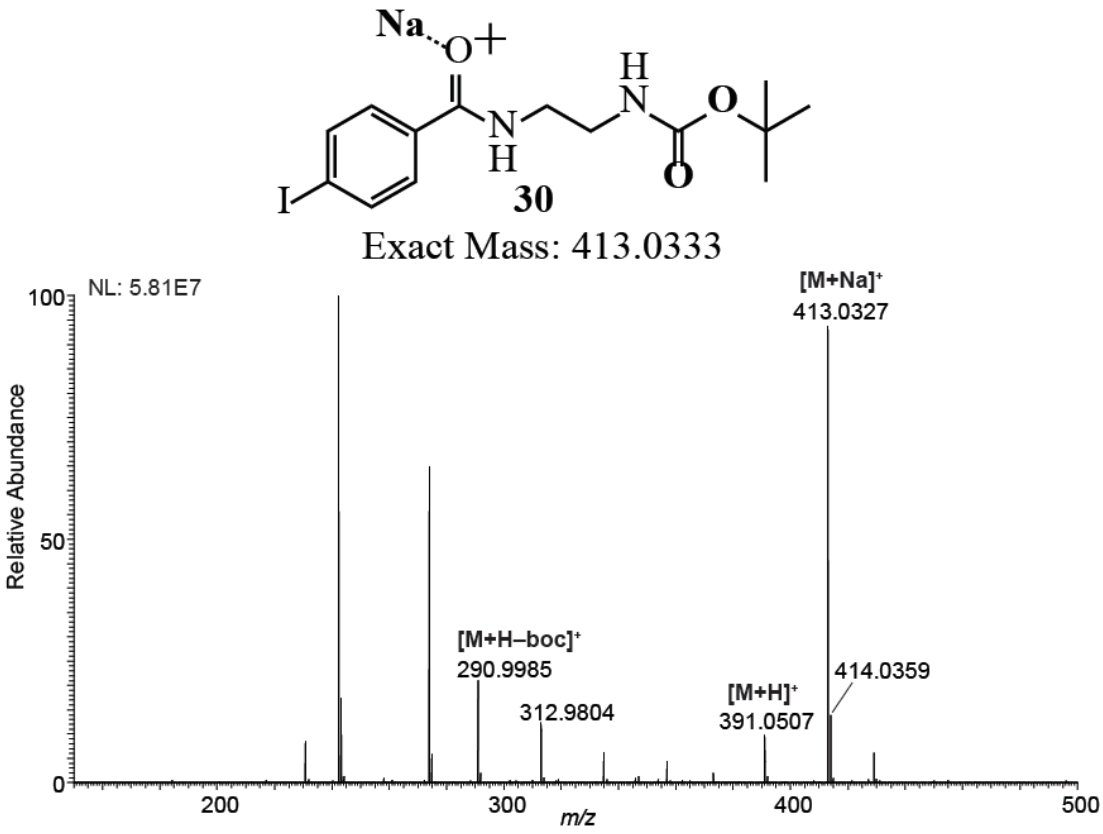

Figure S19: ^{1}H NMR spectra of TFA salt of N-(2-aminoethyl)-4-iodobenzamide (**23**).

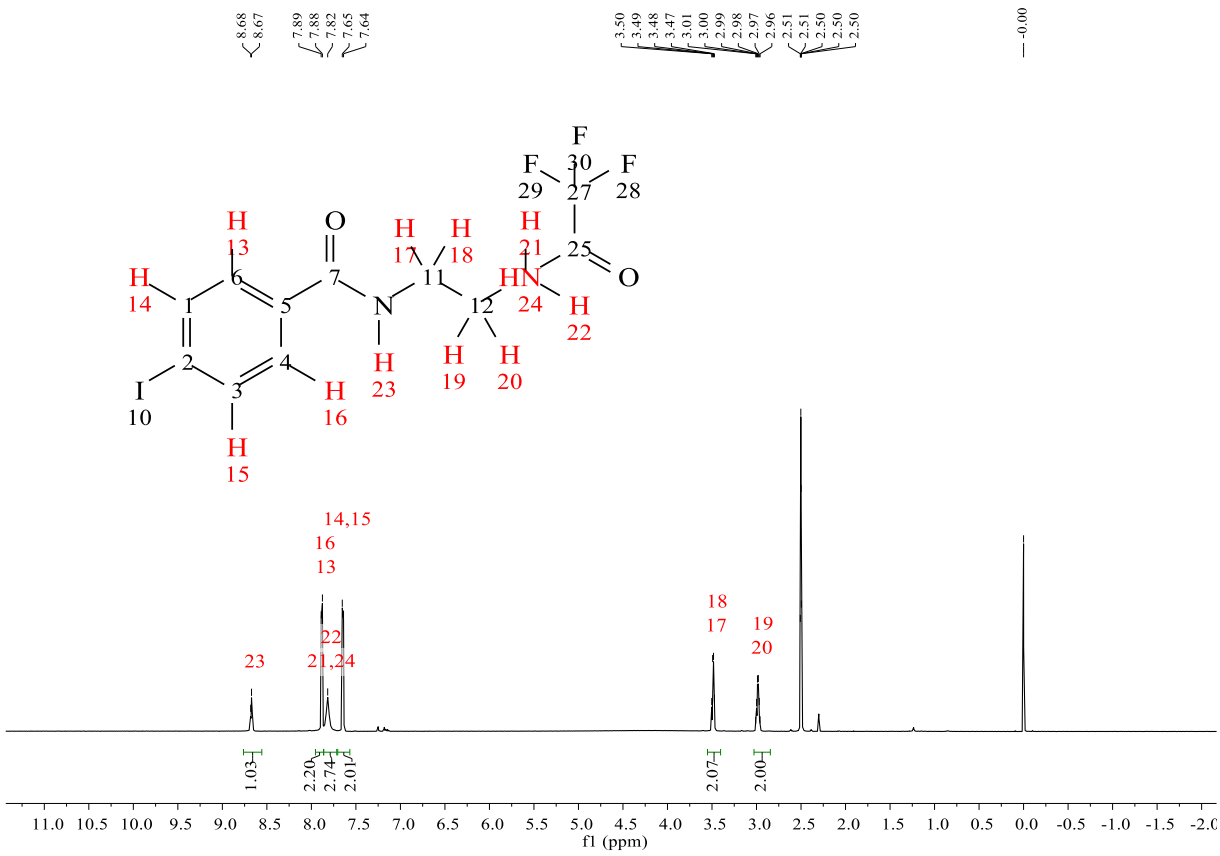

Figure S20: Positive mode ESI-HRMS spectrum of TFA salt of *N*-(2-aminoethyl)-4-iodobenzamide (**23**).

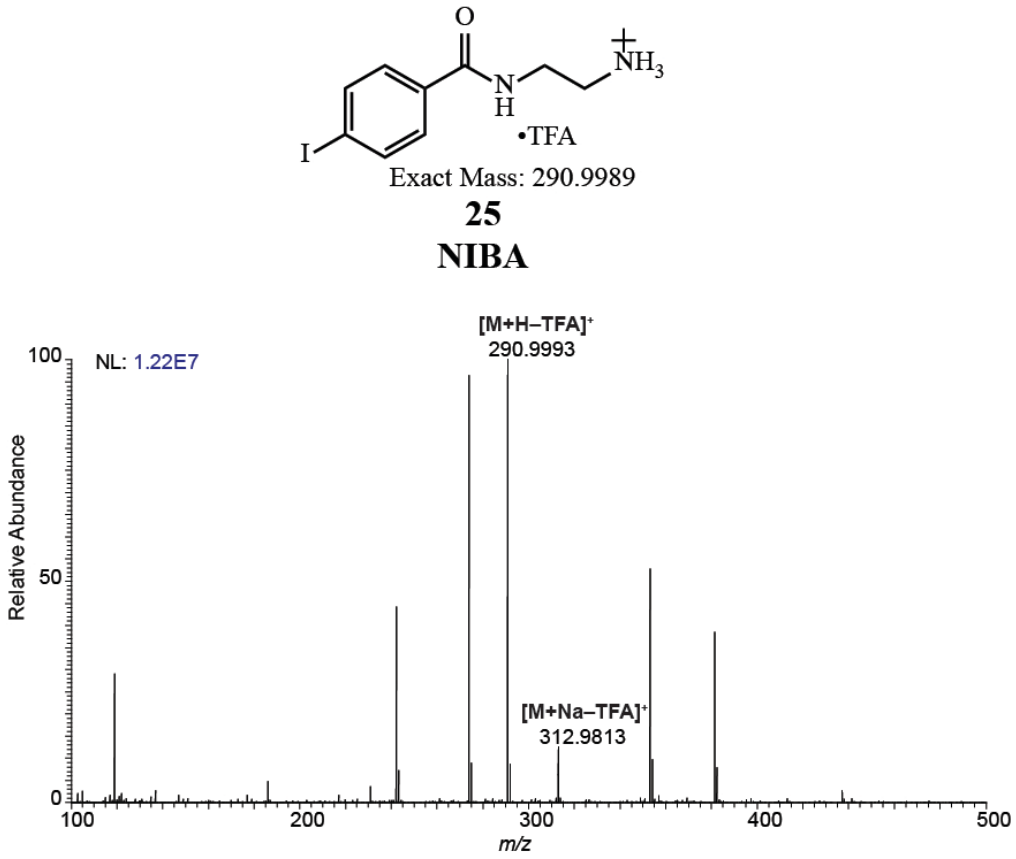

References

1. T. Ly and R. R. Julian, *Journal of the American Chemical Society,* 2008, **130**, 351-358.
2. T. Ly, B. B. Kirk, P. I. Hettiarachchi, B. L. Poad, A. J. Trevitt, G. da Silva and S. J. Blanksby, *Physical Chemistry Chemical Physics,* 2011, **13**, 16314-16323.
3. C. S. Hansen, B. B. Kirk, S. J. Blanksby, R. A. O'Hair and A. J. Trevitt, *Journal of The American Society for Mass Spectrometry,* 2013, **24**, 932-940.
4. F. Neese, *Wiley Interdisciplinary Reviews: Computational Molecular Science,* 2012, **2**, 73-78.
5. F. Neese, *Wiley Interdisciplinary Reviews: Computational Molecular Science,* 2018, **8**, e1327.
6. Y. Zhao and D. G. Truhlar, *Theoretical Chemistry Accounts: Theory, Computation, and Modeling (Theoretica Chimica Acta),* 2008, **120**, 215-241.
7. F. Weigend and R. Ahlrichs, *Physical Chemistry Chemical Physics,* 2005, **7**, 3297-3305.
8. F. Weigend, *Physical chemistry chemical physics,* 2006, **8**, 1057-1065.
9. M. D. Hanwell, D. E. Curtis, D. C. Lonie, T. Vandermeersch, E. Zurek and G. R. Hutchison, *Journal of cheminformatics,* 2012, **4**, 17.
10. O. Christiansen, H. Koch and P. Jørgensen, *Chemical Physics Letters,* 1995, **243**, 409-418.
11. S. Grimme, *The Journal of chemical physics,* 2003, **118**, 9095-9102.
12. TURBOMOLE V7.2 2017, a development of University of Karlsruhe and Forschungszentrum Karlsruhe GmbH, 1989-2009, TURBOMOLE GmbH, since 2007; available from http://www.turbomole.com.
13. C. Hättig and F. Weigend, *The Journal of Chemical Physics,* 2000, **113**, 5154-5161.
14. C. Steffen, K. Thomas, U. Huniar, A. Hellweg, O. Rubner and A. Schroer, *Journal of computational chemistry,* 2010, **31**, 2967-2970.
15. X. Qian, L. Ashcraft, J. Wang, B. Yao, H. Jiang, G. Bergnes, J. C. Huang, J. Wang, B. Morgan, D. Morgans, D. Dhanak, S. Knight, N. Adams, C. Parrish, K. Duffy, D. Fitch and R. Tedesco, 2007.
16. J. F. Poletto, D. W. Powell and D. H. Boschelli, 6th Nov., 1990.
17. H. L. Chan, L. Lyu, J. Aw, W. Zhang, J. Li, H.-H. Yang, H. Hayashi, S. Chiba and B. Xing, *ACS Chem. Biol.,* 2018, **13**, 1890-1896.
18. H. Wu, C. J. Kelley, A. Pino-Figueroa, H. D. Vu and T. J. Maher, *Bioorg. Med. Chem.,* 2013, **21**, 5188-5197.